

Theory of upper critical field, fluctuation conductivity, and fluctuation specific heat for high- T_c superconductors in a magnetic field

C. T. Rieck, Th. Wölkhausen, D. Fay, and L. Tewordt

*Abteilung für Theoretische Festkörperphysik, Universität Hamburg, Jungiusstrasse 11,
D-2000 Hamburg 36, West Germany*

(Received 27 July 1988)

Within the general framework of Bardeen-Cooper-Schrieffer pairing theory we derive coupled gap equations of the Helfand-Werthamer type for two or more order-parameter components having different symmetry. Assuming, for instance, coupled s - and d -wave pairing components, we obtain for certain parameter values a solution for H_{c2} perpendicular to the Cu-O planes which accounts qualitatively for the observed upward curvature and yields about 65 T at zero temperature. We calculate also the in-plane fluctuation conductivity of the Lawrence-Doniach type for fields parallel to the c axis. For large fields, the inverse fluctuation conductivity is almost linear in temperature with slope depending sensitively on the ratio of coherence length to unit-cell dimension along the c axis. It seems possible to fit the observed broad resistive transition for different fields with this inverse fluctuation conductivity. Just above the transition temperature, $T_{c2}(H)$, the inverse ac fluctuation conductivity is approximately a linear function of frequency for small fields, and it is nearly a quadratic function of frequency for large fields. The field dependence of the fluctuation contribution to the specific heat is also discussed in connection with recent measurements.

I. INTRODUCTION

Single crystals¹⁻³ and oriented films⁴ of high- T_c superconductors such as $\text{YBa}_2\text{Cu}_3\text{O}_{7-x}$ show some unusual features in a magnetic field in comparison to ordinary type-II superconductors. The upper critical field and the width of the resistive transition are strongly anisotropic as functions of the angle between the directions of \mathbf{H} and the c axis (the Cu-O sheets are parallel to the ab plane and the c axis is normal to the Cu-O sheets). From the measured slopes of H_{c2} one estimates³ coherence lengths $\xi_{ab}(0) \approx 22 \text{ \AA}$ and $\xi_c(0) \approx 2-4 \text{ \AA}$. For a given field direction H_{c2} shows an upward curvature as T decreases below T_c . The resistive transition in a field is rather broad, in particular for \mathbf{H} lying parallel to the c axis.

Possible explanations for the upward curvature of H_{c2} are critical fluctuations⁵ or flux creep.⁶ The observed curvature of H_{c2} perpendicular to the Cu-O sheets^{3,4} is proportional to $(T_c - T)^{1.35}$ which is in good agreement with the predicted curvature derived from the fluctuation model of Ref. 5, i.e., $(T_c - T)^{1.34}$. On the other hand, the flux creep model predicts a $(T_c - T)^{1.5}$ dependence for H_{c2} which is in general agreement with the observed curvature for H_{c2} parallel to the Cu-O planes.³

Although strong arguments have been given that the observed upward curvature of H_{c2} is caused by critical fluctuations⁵ or by flux creep⁶ we shall, nevertheless, propose in this paper another mechanism, namely, a mixing of pairing components having different symmetries and T_c 's. Our theory is quite analogous to the modified Helfand-Werthamer theory of Scharnberg and Klemm^{7,8} where it has been shown for a special state of partially broken symmetry (a mixing of a p -wave component along and another perpendicular to the c axis) that H_{c2} perpendicular to the c axis can exhibit upward curvature. We re-

mark that the temperature variation of two p -wave pairing components with different T_c 's and their collective mode spectrum become rather complex.⁹ In this paper we shall consider a mixing of an s - and d -wave pairing component similar to the two-component order-parameter model which has been used by Kumar and Wölfle¹⁰ to describe thorium-doped UBe_{13} .

To explain the other field effect on high- T_c superconductors, i.e., the rather broad resistive transition in a field^{1,2,4} we assume that this effect is caused by fluctuation conductivity of the Aslamazov-Larkin and Lawrence-Doniach type. We calculate the fluctuation conductivity from expressions which are analogous to those derived by Klemm.¹¹ Klemm's theory is a generalization of the Lawrence-Doniach theory for layered superconductors¹² where the field effects have been introduced in analogy to the theory of Mikeska and Schmidt¹³ for bulk superconductors in the dirty limit. Here again the flux-creep model^{3,6} offers another explanation, i.e., that the point of deviation of the resistivity from its normal-state value represents $T_c(H)$. This is in accordance with recent reversible measurements of the magnetization¹⁴ which yield an apparent transition temperature that is not suppressed with magnetic field nearly as rapidly as the temperature of zero resistivity which we call $T_{c2}(H)$. We assume that the latter temperature is given by that temperature at which a pole first occurs in the pair fluctuation propagator. This pole corresponds to the lowest Landau level. For \mathbf{H} lying parallel to the c axis this transition temperature is given by¹⁵ $\ln[T_{c2}(H)/T_c] = -\xi_{ab}(0)^2 2eH$. Doubts about the applicability of the Lawrence-Doniach theory have been raised by recent measurements of the in-plane paraconductivity in zero field.¹⁶ It is found that the decrease to zero resistance for $T \rightarrow T_c$ is much more abrupt than described by the $(T - T_c)^{1/2}$ behavior of the Lawrence-

Doniach theory beyond the crossover from two-dimensional (2D) to three-dimensional (3D) behavior. However, we will show that consideration of a second-neighbor tight-binding term along the c axis can give a better fit to the zero-field paraconductivity data.

In this paper we take the point of view that the existing theories for the upper critical field of coupled order-parameter components^{7,8} and for the field effects on the fluctuation conductivity of layered superconductors¹¹ can be applied to describe high- T_c superconductivity. However, we modify these theories to take into account the quasi two dimensionality of the effective tight-binding band and to allow for anisotropic pairing. This is done in analogy to the previous calculation of the coherence lengths and the fluctuation conductivity in zero field.¹⁷ In analogy to the method used for heavy-fermion superconductors,⁹ we expand the order parameter as well as the pairing interaction in terms of basis functions of the representations of the orthorhombic symmetry group.¹⁸ The spatial dependence of the order-parameter components in a field is taken into account by making an expansion in terms of generalized Abrikosov solutions.⁷ The parameters of the theory can be calculated from microscopic theory by assuming an effective 2D band¹⁹ plus a tight-binding band

term along the c axis. We shall see that we can explain qualitatively the observed upward curvature of H_{c2} and the broad resistive transition in a field in terms of our simple model calculations. We find interesting field and frequency dependence of the ac fluctuation conductivity which suggest measurements at microwave and infrared frequencies. Our results for the field dependence of the fluctuation specific heat are discussed in connection with recent measurements.

In Sec. II we develop the theory of the upper critical field for mixed order-parameter components. In Sec. III we calculate the dc and ac fluctuation conductivity for fields parallel to the c axis. The results of Secs. II and III and the fluctuation specific heat are discussed in Sec. IV.

II. THEORY OF UPPER CRITICAL FIELD FOR MIXED ORDER-PARAMETER COMPONENTS

Our starting point is the linearized gap equation for the order parameter $\Delta(\mathbf{r}, \mathbf{k})$ in a magnetic field where \mathbf{r} is the center-of-mass coordinates of the Cooper pair [see Eq. (B4) of Ref. 7]:

$$\Delta(\mathbf{r}, \mathbf{k}) = T \sum_{\omega_n} \int \frac{d^3 k'}{(2\pi)^3} V(\mathbf{k}, \mathbf{k}') \sum_{m=0}^{\infty} \frac{[\nabla_{\mathbf{k}'} \epsilon(\mathbf{k}') \cdot \Pi(\mathbf{r})]^m}{[\epsilon(\mathbf{k}') - i\omega_n][\epsilon(\mathbf{k}') + i\omega_n]^{m+1}} \Delta(\mathbf{r}, \mathbf{k}'). \quad (1)$$

Here, $\epsilon(\mathbf{k})$ is an effective band function, $\omega_n = (2n+1)\pi T$, and $\Pi = -i\nabla_{\mathbf{r}} + 2e\mathbf{A}(\mathbf{r})$. The order parameter and the pairing interaction $V(\mathbf{k}, \mathbf{k}')$ are expanded in terms of basis functions $\psi_i(\mathbf{k})$ of the representations of the orthorhombic symmetry group:¹⁸

$$\Delta(\mathbf{r}, \mathbf{k}) = \sum_j \Delta_j(\mathbf{r}) \psi_j(\mathbf{k}), \quad V(\mathbf{k}, \mathbf{k}') = \sum_j V_j \psi_j(\mathbf{k}) \psi_j(\mathbf{k}'). \quad (2)$$

Let us consider first the Ginzburg-Landau (GL) equations which are obtained if we keep in Eq. (1) only terms up to second order in the momentum operator Π . By making use of the orthogonality of the ψ_i , we obtain from Eq. (1), with the help of Eq. (2)

$$[\alpha_i \ln(T_{ci}/T)] \Delta_i(\mathbf{r}) = \sum_j \int \frac{d^3 k}{(2\pi)^3} \psi_i(\mathbf{k}) \psi_j(\mathbf{k}) B(\mathbf{k}) [\nabla_{\mathbf{k}} \epsilon(\mathbf{k}) \cdot \Pi(\mathbf{r})]^2 \Delta_j(\mathbf{r}), \quad (3)$$

where

$$\alpha_i \ln(T_{ci}/T) = \int \frac{d^3 k}{(2\pi)^3} \psi_i(\mathbf{k})^2 \left[T \sum_{\omega_n(T)} \frac{|\tilde{\omega}_n|}{|\omega_n| [\tilde{\omega}_n^2 + \epsilon(\mathbf{k})^2]} - T_c \sum_{\omega_n(T_c)} \frac{|\tilde{\omega}_n|}{|\omega_n| [\tilde{\omega}_n^2 + \epsilon(\mathbf{k})^2]} \right], \quad (4)$$

$$B(\mathbf{k}) = \frac{1}{4} T_c \sum_{\omega_n(T_c)} \frac{1}{\omega_n^2} \left[\frac{4\tilde{\omega}_n^4}{[\tilde{\omega}_n^2 + \epsilon(\mathbf{k})^2]^3} - \frac{\tilde{\omega}_n^2}{[\tilde{\omega}_n^2 + \epsilon(\mathbf{k})^2]^2} \right]. \quad (5)$$

The $\tilde{\omega}_n$ denote the renormalized Matsubara frequencies in the presence of impurity scattering.¹⁷

We take as a band model $\epsilon(\mathbf{k}) = \epsilon(k_x, k_y) + t_z [\cos(k_z c) - 1]$ where $\epsilon(k_x, k_y)$ is an effective 2D tight-binding band, for instance, that of Emery,¹⁹ and the second term describes a small band dispersion in the k_z direction. Further, we assume for simplicity only extended s -wave and d -wave pairing in the $xy(ab)$ plane. The corresponding

basis functions are¹⁸

$$\begin{aligned} \psi_1(\mathbf{k}) &= \cos k_x a + \cos k_y a, \\ \psi_2(\mathbf{k}) &= \cos k_x a - \cos k_y a, \\ \psi_3(\mathbf{k}) &= 2 \sin(k_x a) \sin(k_y a). \end{aligned} \quad (6)$$

Mixing of states of different symmetry has been con-

sidered previously for heavy-fermion superconductors, for instance, mixing of two p -wave pairing states⁹ and mixing of an s - and d -wave pairing state.¹⁰ We specialize now to a magnetic field perpendicular to the ab plane. Since we are interested here in the upper critical field H_{c2} , which is given by the largest eigenvalue of Eq. (3), we can assume that $\Delta_i(\mathbf{r})$ is independent of z . Then the kinetic energy operator in the GL Eq. (3) can be separated into three parts, which have the same symmetries as the three ψ_i in Eq. (6):

$$\begin{aligned} [\mathbf{V}_k \epsilon(\mathbf{k}) \cdot \Pi(\mathbf{r})]^2 &= \frac{1}{2} (\epsilon_x^2 + \epsilon_y^2) (\Pi_- \Pi_+ + \Pi_+ \Pi_-) \\ &\quad + \frac{1}{2} (\epsilon_x^2 - \epsilon_y^2) (\Pi_+^2 + \Pi_-^2) \\ &\quad - \epsilon_x \epsilon_y i (\Pi_+^2 - \Pi_-^2), \end{aligned} \quad (7)$$

$$\Pi_{\pm} = \frac{1}{\sqrt{2}} (\Pi_x \pm i \Pi_y), \quad \epsilon_v = (\partial / \partial k_v) \epsilon(\mathbf{k}). \quad (8)$$

The gap functions $\psi_i(\mathbf{r})$ are expanded now in terms of the complete set of generalized Abrikosov solutions (Ref. 7) $g_N(\mathbf{r})$, with $p_z = 0$, $\mathbf{r} = x, y$, and $N = 0, 1, 2, \dots$ being the harmonic-oscillator quantum numbers

$$\begin{aligned} \Delta_1(\mathbf{r}) &= \sum_N b_N g_N(\mathbf{r}), \\ \Delta_2(\mathbf{r}) &= \sum_N c_N g_N(\mathbf{r}), \\ \Delta_3(\mathbf{r}) &= \sum_N i d_N g_N(\mathbf{r}), \\ \Pi_+ g_N &= (2eH)^{1/2} (N+1)^{1/2} g_{N+1}, \\ \Pi_- g_N &= (2eH)^{1/2} N^{1/2} g_{N-1}. \end{aligned} \quad (9)$$

One recognizes that in the GL equation (3), the second term of the operator in Eq. (7) gives rise to coupling between Δ_1 and Δ_2 , and the third term in Eq. (7) leads to a coupling between Δ_1 and Δ_3 .

By inserting Eqs. (6)–(10) into Eq. (3) we obtain three sets of coupled equations where the first set contains the coefficients $b_N, c_{N-2}, c_{N+2}, d_{N-2}, d_{N+2}$ ($N = 0, 2, 4, \dots$), the second set contains c_N, b_{N-2}, b_{N+2} , and the third set contains d_N, b_{N-2} , and b_{N+2} . Three types of coefficients occur in these equations which arise from the three parts

of the operator in Eq. (7):

$$\begin{aligned} \eta_i a^2 &= \int d^2 k (2\pi)^{-2} \psi_i(\mathbf{k})^2 B(\mathbf{k})^{\frac{1}{2}} (\epsilon_x^2 + \epsilon_y^2), \\ \eta_{12} a^2 &= \int d^2 k (2\pi)^{-2} \psi_1(\mathbf{k}) \psi_2(\mathbf{k}) B(\mathbf{k})^{\frac{1}{2}} (\epsilon_x^2 - 0 \epsilon_y^2), \\ \eta_{13} a^2 &= \int d^2 k (2\pi)^{-2} \psi_1(\mathbf{k}) \psi_3(\mathbf{k}) B(\mathbf{k}) \epsilon_x \epsilon_y. \end{aligned} \quad (11)$$

The η_i are related to the GL coherence lengths by

$$\xi_i(T)^2 = \xi_i(0)^2 [T_{ci} / (T_{ci} - T)]$$

where $\xi_i(0)^2 = (\eta_i / a_i) a^2$. The quantities η_{12} and η_{13} are the coupling terms between Δ_1 and Δ_2 , and Δ_1 and Δ_3 , respectively.

It is interesting to consider the generalized GL equations which have been successfully applied for conventional superconductors to obtain correction terms to GL of order $(T_c - T) / T_c$. The generalized GL equations are obtained from Eq. (1) by taking into account fourth-order terms in Π . Again the operator $[\mathbf{V}_k \epsilon(\mathbf{k}) \cdot \Pi(\mathbf{r})]^4$ can be separated into three parts whose coefficients have the same properties with respect to symmetry operations in \mathbf{k} space, as the basis functions in Eq. (6) or the coefficients in Eq. (7). Therefore, this operator leads again to couplings between Δ_1 and Δ_2 , and Δ_1 and Δ_3 , respectively. The first set of equations for the coefficients in Eq. (9) contains now $b_N, b_{N-4}, b_{N+4}, c_{N-2}, c_{N+2}, d_{N-2}, d_{N+2}$ ($N = 0, 2, 4, \dots$), and two corresponding sets with $b_N \leftrightarrow c_N$ and $b_N \leftrightarrow d_N$, respectively. For lack of space we cannot write down these equations.

In order to obtain coupled order-parameter equations, which are valid at all temperatures and fields, we now make the following drastic approximation. We integrate in Eq. (1) over $\epsilon(\mathbf{k}')$ from $-\infty$ to $+\infty$ at fixed direction of \mathbf{k}' . By numerical computations, we have ascertained that for the Emery band¹⁹ the integrand is sharply peaked at the Fermi surface, $\epsilon(\mathbf{k}') = 0$. We now expand the order parameter $\Delta(\mathbf{r}, \hat{\mathbf{k}})$ ($\hat{\mathbf{k}} = \mathbf{k} / |\mathbf{k}|$) and the pairing interaction in analogy to Eq. (2) in terms of basis functions $\psi_i(\hat{\mathbf{k}})$. The s - and d -wave functions corresponding to Eq. (6) are

$$\begin{aligned} \psi_1(\hat{\mathbf{k}}) &= (\hat{\mathbf{k}}_x^2 + \hat{\mathbf{k}}_y^2), \\ \psi_2(\hat{\mathbf{k}}) &= \sqrt{2} (\hat{\mathbf{k}}_x^2 - \hat{\mathbf{k}}_y^2), \\ \psi_3(\hat{\mathbf{k}}) &= \sqrt{8} \hat{\mathbf{k}}_x \hat{\mathbf{k}}_y. \end{aligned} \quad (12)$$

In this way we obtain from Eq. (1), approximately, the following coupled Helfand-Werthamer equations:

$$\Delta_i(\mathbf{r}) = V_i N(0) \sum_j \int \frac{d\Omega_k}{4\pi} \psi_i(\hat{\mathbf{k}}) \psi_j(\hat{\mathbf{k}}) \pi T \sum_{\omega_n} \int_0^{\infty} dt \exp(-|\omega_n|t) \exp[-t(i/2)(\text{sgn} \omega_n) \mathbf{V}_k \epsilon(\mathbf{k}) \cdot \Pi(\mathbf{r})] \Delta_j(\mathbf{r}), \quad (13)$$

where $N(0)$ is an effective density of states and $\mathbf{V}_k \epsilon(\mathbf{k})$ is at the Fermi surface.

We again assume $\mathbf{H} \parallel \hat{\mathbf{z}}$, and that Δ_j does not depend on z . The exponential operator is written in the usual form in terms of Boson creation and annihilation operators c^\dagger and c :

$$\exp[-t(i/2) \text{sgn} \omega_n \mathbf{V}_k \epsilon \cdot \Pi] = \exp[\frac{1}{2} it (\eta c^\dagger + \eta^* c)], \quad (14)$$

$$c^{(+)} = (4eH)^{-1/2} (\Pi_x \frac{(+)}{-} i \Pi_y) = (2eH)^{-1/2} \Pi_{(+)} \eta = -(\text{sgn} \omega_n) (eH)^{1/2} (\epsilon_x - i \epsilon_y).$$

The matrix elements of this operator with respect to the states $g_N(\mathbf{r})$ ($\mathbf{r} = x, y; p_z = 0$) can be expressed in terms of associated Laguerre polynomials L_n^m (see Ref. 20):

$$\langle N' | \exp[\frac{1}{2} it(\eta c^\dagger + \eta^* c)] | N \rangle = \exp(-\frac{1}{4} t^2 |\eta|^2) (\frac{1}{2} it \eta^*)^{N-N'} (N!/N!)^{1/2} L_N^{N-N'} (\frac{1}{4} t^2 |\eta|^2) \quad (N \geq N'),$$

$$|\eta(\hat{\mathbf{k}})|^2 = eH(\epsilon_x^2 + \epsilon_y^2).$$

For $N' \geq N$, $\eta^* \rightarrow \eta$ and $N \leftrightarrow N'$.

By inserting Eqs. (9), (14), and (15) into Eq. (13) we obtain three sets of coupled equations for the coefficients b_N , c_N , and d_N . The problem now is to carry out the integrations over the solid angle $d\Omega_k$. Since, for our band model, ϵ_x and ϵ_y and thus $\eta(\hat{\mathbf{k}})$ depend only on $\hat{\mathbf{k}}_x$ and $\hat{\mathbf{k}}_y$, and since the pairing functions in Eq. (12) depend only on $\hat{\mathbf{k}}_x$ and $\hat{\mathbf{k}}_y$, we have to carry out a single integration over the azimuthal angle ϕ . Most important are the terms $[\eta^*(\hat{\mathbf{k}})]^{N-N'}$ in Eq. (15) which generate the couplings between different states. We shall approximate $|\eta(\hat{\mathbf{k}})|^2$ by appropriate averages over the angle ϕ from zero to 2π which depend on the weighting functions $\psi_i(\hat{\mathbf{k}})\psi_j(\hat{\mathbf{k}})$. In this way we obtain the following sets of coupled equations for $N=0,2,4,\dots$ (for brevity we omit the coefficients d_N):

$$\left[[V_1 N(0)]^{-1} - \pi T \sum_{\omega_n} \int_0^\infty dt \exp(-|\omega_n|t - \frac{1}{8} t^2 eHv_1^2) L_N^0(\frac{1}{4} t^2 eHv_1^2) \right] b_N$$

$$+ \left[\pi T \sum_{\omega_n} \int_0^\infty dt \exp(-|\omega_n|t - \frac{1}{8} t^2 eHv_1^2) \frac{1}{\sqrt{2}} (\frac{1}{4} t^2 eHv_1^2) \right. \\ \left. \times \{ [(N+2)(N+1)]^{-1/2} L_N^2(\frac{1}{4} t^2 eHv_1^2) c_{N+2} + [N(N-1)]^{-1/2} L_{N-2}^2(\frac{1}{4} t^2 eHv_1^2) c_{N-2} \} \right] = 0,$$

(16)

$$\left[[V_2 N(0)]^{-1} c_N - \pi T \sum_{\omega_n} \int_0^\infty dt \exp(-|\omega_n|t - \frac{1}{8} t^2 eHv_2^2) \right. \\ \left. \times (L_N^0(\frac{1}{4} t^2 eHv_2^2) c_N + \frac{1}{2} (\frac{1}{4} t^2 eHv_2^2)^2 \{ [(N+4)(N+3)(N+2)(N+1)]^{-1/2} L_N^4(\frac{1}{4} t^2 eHv_2^2) c_{N+4} \right. \\ \left. + [N(N-1)(N-2)(N-3)]^{-1/2} L_{N-4}^4(\frac{1}{4} t^2 eHv_2^2) c_{N-4} \} \right) \\ + \left[\pi T \sum_{\omega_n} \int_0^\infty dt \exp(-|\omega_n|t - \frac{1}{8} t^2 eHv_2^2) \frac{1}{\sqrt{2}} (\frac{1}{4} t^2 eHv_2^2) \right. \\ \left. \times \{ [(N+2)(N+1)]^{-1/2} L_N^2(\frac{1}{4} t^2 eHv_2^2) b_{N+2} + [N(N-1)]^{-1/2} L_{N-2}^2(\frac{1}{4} t^2 eHv_2^2) b_{N-2} \} \right] = 0.$$

(17)

As has been pointed out above, the $v_i^2 = v_{ii}^2$ and v_{ij}^2 are averages of $|\nabla_k \epsilon(\mathbf{k})|^2$ over the Fermi line perpendicular to \mathbf{H} , which refer to the different weighting functions $\psi_i(\hat{\mathbf{k}})\psi_j(\hat{\mathbf{k}})$ in Eq. (13). We shall consider, in the following, the v_i^2 and v_{ij}^2 as parameters of the theory. The other parameters are the pairing interaction constants V_i which can be expressed in terms of different transition temperatures T_{ci} by means of the zero-field gap equations. Then Eqs. (16) and (17) can be rewritten in terms of the following reduced quantities:

$$h = eH(v_1/2\pi T_{c1})^2,$$

$$t = T/T_{c1}, \quad (T_{c2}/T_{c1}), \quad (v_1/v_1)^2, \quad (v_{12}/v_1)^2. \quad (18)$$

The ratio T_{c2}/T_{c1} is related to the pairing interaction constants by

$$\ln(T_{c2}/T_{c1}) = [N(0)V_1]^{-1} - [N(0)V_2]^{-1}.$$

The averages of the squared Fermi velocities v_{ij}^2 can be related to the coefficients η_{ij} of the GL equations in Eq. (11). These relations are obtained by expanding Eqs.

(16) and (17) in powers of $(eH)^{1/2} v_{ij}/2|\omega_n|$ and comparing the first two terms of this expansion with the GL equations in Eq. (3). This yields the relationship

$$\eta_{ij} a^2 = [7\zeta(3)/32\pi^2 T_{ci}^2] v_{ij}^2. \quad (19)$$

Thus, we can calculate in principle the parameters $(v_2/v_1)^2$ and $(v_{12}/v_1)^2$ for a particular 2D band with the help of Eqs. (19) and (11).

We have solved the secular equation for the system of linear Eqs. (16) and (17) for $b_0, c_2, b_4, c_6, \dots$, up to b_{12} . There exist many solutions for $h(t)$ and the largest yields $h_{c2}(t)$. We present our numerical results for $h_{c2}(t)$ in terms of $h_{c2}^*(t)$, which is the reduced upper critical field [see Eq. (18)] normalized to its slope at $t=1$:

$$h_{c2}^*(t) = h_{c2}(t) [|dh_{c2}(t)/dt|_{t=1}]^{-1}. \quad (20)$$

In Fig. 1 we show our numerical results for $h_{c2}^*(t)$ vs t for parameter values $T_{c2}/T_{c1}=0.92$, $(v_2/v_1)^2=1.9$, and $(v_{12}/v_1)^2=1.4$ [curve (1)]. The points in Fig. 1 represent the experimental points found by Worthington *et al.*³ One sees that the observed upward curvature of H_{c2} is

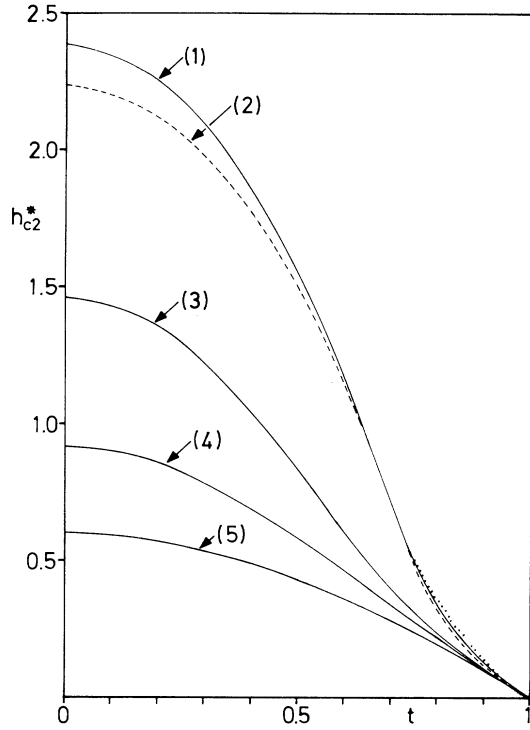


FIG. 1. The reduced upper critical field parallel to the c axis $h_{c2}^*(t)$ [see Eq. (20)], vs $t = T/T_{c1}$. The curves denoted by (1)–(5) refer to a mixed s - and d -wave pairing state with parameters T_{c2}/T_{c1} , $(v_2/v_1)^2$, and $(v_{12}/v_1)^2$ (the v 's are effective Fermi velocities). The parameter values are $T_{c2}/T_{c1} = 0.92$ for (1), and $T_{c2}/T_{c1} = 1$ for (2)–(5); $(v_2/v_1)^2 = 1.9$ for (1)–(3) and (5), and 1.5 for (4); $(v_{12}/v_1)^2 = 1.4$ for (1) and (2), 1.2 for (3) and (4), and 0 for (5). The dots represent the experimental data of Ref. 3.

simulated reasonably well by our theoretical curve. At zero temperature, we obtain with the help of Eq. (20) an upper critical field

$$H_{c2}(0) \simeq h_{c2}^*(0)(0.3T/K)92.6 \text{ K} \simeq 66 \text{ T}$$

which is close to the estimate of 64 T given in Ref. 3. Curve (5) represents $h_{c2}^*(t)$ for a pure pairing state ($T_{c2}/T_{c1} = 1$, $v_2 = v_{12} = 0$). Notice that for the two-dimensional case $h_{c2}^*(0) = 0.6$, which should be compared with the well-known value of 0.72 for the three-dimensional case (clean limit).

We have calculated the quantities η_{ij} from Eq. (11) by using the Emery-band¹⁹ and s - and d -wave pairing states [see Eq. (6)]. Then we find with the help of the relationship in Eq. (19) that the parameter values for $(v_2/v_1)^2$ and $(v_{12}/v_1)^2$ used to obtain curve (1) in Fig. 1 are quite realistic. The $h_{c2}^*(t)$ is insensitive to T_{c2}/T_{c1} and it is sensitive to the values of $(v_2/v_1)^2$ and in particular to the values of the coupling strength $(v_{12}/v_1)^2$ [see curves (2)–(5) in Fig. 1].

III. THEORY OF FLUCTUATION CONDUCTIVITY FOR LAYERED SUPERCONDUCTORS IN A FIELD

The Aslamazov-Larkin (AL) contribution to the fluctuation conductivity in zero field has been calculated previously¹⁷ by taking into account the quasi two dimensionality of the tight-binding band [$\epsilon(k_x, k_y)$] and of the superconducting wave function. A small band-dispersion term in the z direction [$t_z(\cos k_z c - 1)$] yields essentially the Lawrence-Doniach fluctuation conductivity¹² giving rise to a crossover from 2D to 3D behavior as $T \rightarrow T_c$. The pair fluctuation propagator $K(\mathbf{q}, \omega)$ is then found to be

$$K^{-1}(\mathbf{q}, \omega) = \{ \alpha \ln(T/T_c) + 4\eta_{x,y} [\sin^2(q_x a/2) + \sin^2(q_y a/2)] + 4\eta_z \sin^2(q_z c/2) - i\tau\omega \}. \quad (21)$$

Here, $-\alpha \ln(T/T_c)$ and $\eta_{x,y}$ are given by Eqs. (4) and (11) (from now on we omit the subscript i referring to the pairing state). The coefficient η_z is obtained from the expression for $\eta_{x,y}$ [see Eq. (11)] by replacing $(\epsilon_x^2 + \epsilon_y^2)/2$ by $\frac{1}{8} t_z^2 a^2$. The relaxation time τ is given by

$$\tau = (\pi/2) \int d^2 k (2\pi)^{-2} \psi(\mathbf{k})^2 [2\epsilon(\mathbf{k})]^{-1} \tanh[\epsilon(\mathbf{k})2T_c] \delta[\epsilon(\mathbf{k})]. \quad (22)$$

The effect of a field can be calculated from the eigenvalues of a certain differential operator of infinite order [see Eq. (A7) of Ref. 15] whose kernel contains the Fourier transform of $K^{-1}(\mathbf{q}, \omega)$. For a field H parallel to the z axis, these eigenvalues can easily be calculated if one expands $K^{-1}(\mathbf{q}, \omega)$ in powers of q_x^2 and q_y^2 and keeps only the first-order terms. This has the effect that $(q_x^2 + q_y^2)$ is replaced by the eigenvalues $2eH(2N+1)$ of the Landau states having harmonic-oscillator quantum numbers $N = 0, 1, 2, \dots$. In this way we find that the inverse fluctuation propagator in Eq. (21) is replaced by

$$K_N^{-1}(q_z, \omega) = \alpha \{ \ln(T/T_c) + \xi_{x,y}(0)^2 (2eH)(2N+1) + 4[\xi_z(0)/c]^2 \sin^2(q_z c/2) - i\tau\omega \}, \quad (23)$$

where

$$\xi_{x,y}(0)^2 = \eta_{x,y} a^2 / \alpha, \quad \xi_z(0)^2 = \eta_z c^2 / \alpha. \quad (24)$$

The two current operators occurring at the vertices of the AL diagram cause transitions between Landau levels $N \rightarrow N+1$ and vice versa. Mikeska and Schmidt¹³ have calculated the fluctuation conductivity of a bulk superconductor in a field for the dirty limit, and Klemm¹¹ has generalized their calculation to layered superconductors. Following the methods of Refs. 13 and 11 and using our fluctuation propagator in Eq. (23) we obtain for the average AL fluctuation conductivity in the $xy(ab)$ plane for a field \mathbf{H} lying in the $z(c)$ direction:

$$\sigma'_H(\omega) = \frac{e^2 \bar{\tau}}{16 \hbar c} h^2 \sum_{N=0}^{\infty} 4(N+1) \int_{-\pi}^{+\pi} \frac{d\phi}{2\pi} \frac{\Gamma_N(\phi) + \Gamma_{N+1}(\phi)}{\Gamma_N(\phi) \Gamma_{N+1}(\phi)} \left\{ \frac{1}{4} [\Gamma_N(\phi) + \Gamma_{N+1}(\phi)]^2 + (\bar{\tau}\bar{\omega})^2 \right\}^{-1}, \quad (25)$$

where

$$\begin{aligned} \Gamma_N(\phi) &= [\epsilon_h + 2hN + \frac{1}{2} \gamma(1 - \cos\phi)], \\ \epsilon_h &= \ln[T/T_{c2}(H)] = \epsilon + h, \quad \epsilon = \ln(T/T_c), \\ h &= \xi_{x,y}(0)^2 2eH, \quad \gamma = 4[\xi_z(0)/c]^2, \\ \bar{\omega} &= \pi \hbar \omega / 16 k_B T_c, \quad \bar{\tau} = 8 k_B T_c \tau / \pi \hbar \alpha. \end{aligned} \quad (26)$$

In Eq. (25) the integration over the angle ϕ can be carried out and we obtain

$$\begin{aligned} \sigma'_H(\omega) &= (e^2 \bar{\tau} / 16 \hbar c) \tilde{\sigma}_h(\bar{\tau}\bar{\omega}), \\ \tilde{\sigma}_h(\bar{\tau}\bar{\omega}) &= 4h^2 [h^2 + (\bar{\tau}\bar{\omega})^2]^{-1} \\ &\quad \times \sum_{N=0}^{\infty} (N+1) \left\{ [(\epsilon_h + 2hN)(\epsilon_h + 2hN + \gamma)]^{-1/2} + [(\epsilon_h + 2h(N+1))(\epsilon_h + 2h(N+1) + \gamma)]^{-1/2} \right. \\ &\quad \left. - 2 \{ [\epsilon_h + 2h(N + \frac{1}{2})]^2 + (\bar{\tau}\bar{\omega})^2 \}^{-1/4} \{ [\epsilon_h + 2h(N + \frac{1}{2}) + \gamma]^2 + (\bar{\tau}\bar{\omega})^2 \}^{-1/4} \right. \\ &\quad \left. \times \cos(\frac{1}{2} \arctan\{\bar{\tau}\bar{\omega}/[\epsilon_h + 2h(N + \frac{1}{2})]\}) + \frac{1}{2} \arctan\{\bar{\tau}\bar{\omega}/[\epsilon_h + 2h(N + \frac{1}{2}) + \gamma]\} \right\}. \end{aligned} \quad (28)$$

The limit $\bar{\tau}\bar{\omega} \rightarrow 0$ of the expression in Eq. (28) corresponds to the limit $\omega \rightarrow 0$ of the expression derived in Eq. (10) of Ref. 11 for the dirty limit. However, our expression in Eq. (28) is valid at all frequencies while that of Eq. (10) in Ref. 11 corresponds to an expansion of the integrand in Eq. (25) in powers of ω^2 , up to first order in ω^2 .

Let us consider first the limit $\omega \rightarrow 0$. In Fig. 2(a) we have plotted our numerical results for the inverse reduced fluctuation conductivity $\tilde{\sigma}_h^{-1}(0)$ vs $\epsilon = \ln(T/T_c) = \epsilon_h - h$. For the ratio $\xi_z(0)/c$ we have taken the value $\sqrt{2}/10$ which yields $\gamma = 0.08$. Hagen, Wang, and Ong¹⁶ have tried to fit their in-plane paraconductivity data in zero field for single crystals of YBa₂Cu₃O₇ by the Lawrence-Doniach expression, using values of $\gamma = \nu(0)$ close to 0.08. Oh *et al.*⁴ have used parameter values $\gamma = 0.12, 0.05$, and 0.07 to fit their fluctuation conductivity data obtained on oriented thin films of YBa₂Cu₃O₇ in zero field. Our reduced field values used in Fig. 2(a) range from 0 to 0.18. From the estimate of $\xi_a(0) \approx 24 \text{ \AA}$ of Iye, Tamegai, Takeya, and Takei² together with the expression for the reduced field, $h = \xi_{x,y}(0)^2 2eH$, we approximately obtain $h \approx 0.012H(T)$. The observed decrease of the zero-resistance temperature for H parallel to the c axis varies approximately as $[T_c - T_{c2}(H)]/T_c = h \approx 0.012H(T)$. The highest reduced field used in Fig. 2(a), $h = 0.18$, corresponds to about $H = 15 \text{ T}$.

One recognizes from Fig. 2(a) that $\tilde{\sigma}_h^{-1}(0)$ is zero at $\epsilon_h = 0$ ($\epsilon = -h$) as it should be, and that for larger values

of ϵ_h the curve for $\tilde{\sigma}_h^{-1}$ becomes nearly parallel to the curve for the inverse Lawrence-Doniach conductivity,¹² $\tilde{\sigma}_0^{-1}(0) = [\epsilon(\epsilon + \gamma)]^{1/2}$. Hagen *et al.*¹⁶ find that in zero field, the decrease to zero resistance for decreasing ϵ is much more abrupt than described by the $\epsilon^{1/2}$ behavior [see Fig. 2(a) for $h=0$]. We have generalized the Lawrence-Doniach theory by taking into account a next-nearest-neighbor contribution of the band dispersion term in the z direction such that the total tight-binding band term in the z direction becomes $t_z(\cos ck_z - 1) + t'_z(\cos 2ck_z - 1)$. The resulting inverse-fluctuation conductivity varies as $\tilde{\sigma}_0^{-1} \approx \{[(1+r)/r](\gamma\epsilon)\}^{1/2}$ for $\epsilon \ll \gamma$, and $\tilde{\sigma}_0^{-1} \approx \epsilon + \gamma(\frac{1}{2} + 1/8r)$ for $\epsilon \gg \gamma$ where $r = t_z^2/4t_z'^2$. In order to fit the given paraconductivity data in the ab plane one has to decrease the crossover temperature γ as r becomes finite. The effect is that the corrected curve of $\tilde{\sigma}_0^{-1}$ yields a more abrupt decrease and better fit to the data as ϵ tends to zero. We expect that the corrected curves of $\tilde{\sigma}_h^{-1}$ as functions of ϵ_h will again be nearly parallel to the corrected curves of $\tilde{\sigma}_0^{-1}$ for larger values of ϵ . Qualitatively, the picture will be the same as shown in Fig. 2(a).

We consider now the fluctuation conductivity at finite frequencies given by Eqs. (27) and (28). In Fig. 2(b) we have plotted our numerical results for $\tilde{\sigma}_h^{-1}$ vs $\bar{\tau}\bar{\omega}$ for a fixed reduced temperature $\epsilon_h = 0.001$ and for several values of the reduced field h . In the limit $h \rightarrow 0$, we obtain correctly the curve that has been calculated independently from the following integral [see Eq. (7) of Ref. 17]:

$$\tilde{\sigma}_0(\bar{\tau}\bar{\omega}) = \frac{2}{\bar{\tau}\bar{\omega}} \int_{-\pi}^{+\pi} \frac{d\phi}{2\pi} \left\{ \arctan \left[\frac{\bar{\tau}\bar{\omega}}{\epsilon + \frac{1}{2} \gamma(1 - \cos\phi)} \right] - \frac{1}{2} \left[\frac{\epsilon + (\gamma/2)(1 - \cos\phi)}{\bar{\tau}\bar{\omega}} \right] \ln \left[1 + \left[\frac{\bar{\tau}\bar{\omega}}{\epsilon + (\gamma/2)(1 - \cos\phi)} \right]^2 \right] \right\}. \quad (29)$$

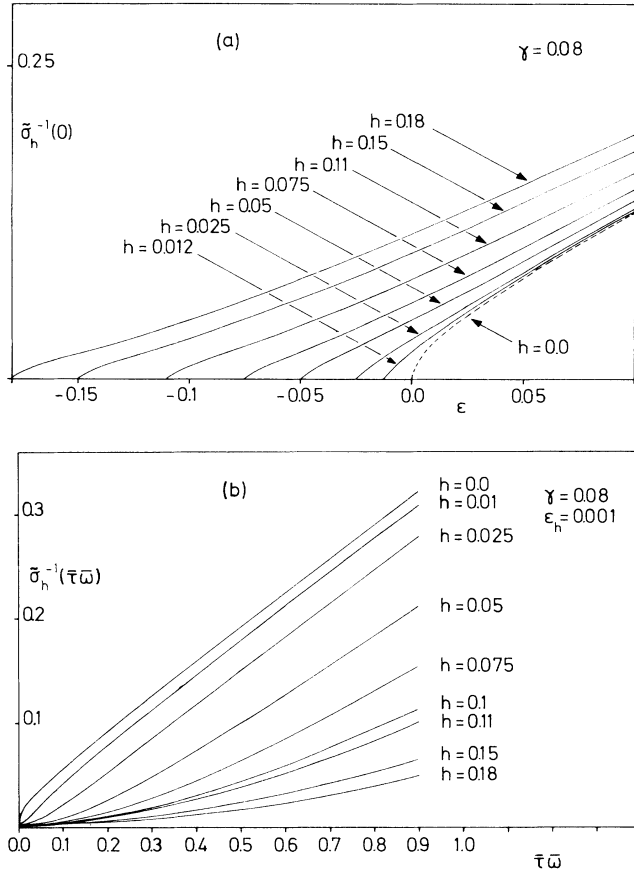


FIG. 2. Inverse of the in-plane reduced fluctuation conductivity $\bar{\sigma}_h^{-1}$ [see Eq. (27)] for different reduced fields h parallel to the c axis and for a 2D to 3D crossover parameter value $\gamma = 4[\xi_z(0)/c]^2 = 0.08$. Approximately, $h = 0.012H(T)$. (a) Inverse of the dc conductivity versus reduced temperature $\epsilon \equiv \ln(T/T_c)$. The following relations hold: $\epsilon = \epsilon_h - h$ where $\epsilon_h \equiv \ln[T/T_{c2}(H)]$. Thus $\bar{\sigma}_h^{-1}(0) = 0$ at $\epsilon = -h$ corresponding to $\epsilon_h = 0$ or $T = T_{c2}(H)$. (b) Inverse of the ac conductivity vs reduced frequency variable $\bar{\tau}\bar{\omega}$ [see Eq. (26)] for $\epsilon_h = 0.001$.

In the limit $\bar{\tau}\bar{\omega} \gg (\epsilon + \gamma)$, Eq. (29) yields

$$\bar{\sigma}_0(\bar{\tau}\bar{\omega}) \sim \pi/\bar{\tau}\bar{\omega} \quad [\bar{\tau}\bar{\omega} \gg (\epsilon + \gamma)], \quad (30)$$

which agrees in the limit $\gamma \rightarrow 0$ and $\epsilon \rightarrow 0$ with the well-known result for an ordinary bulk superconductor. For finite h and $\epsilon_h \ll h$ the first term for $N=0$ in Eq. (28) becomes dominating. This term yields

$$\bar{\sigma}_h(\bar{\tau}\bar{\omega}) \approx \frac{4h^2}{h^2 + (\bar{\tau}\bar{\omega})^2} [\epsilon_h(\epsilon_h + \gamma)]^{-1/2} \quad (h \gg \epsilon_h). \quad (31)$$

Comparison of Eq. (31) with the exact results shown in Fig. 2(b) shows that Eq. (31) is a good approximation only for $\bar{\tau}\bar{\omega} < h$. For $\bar{\tau}\bar{\omega} \gg h$ the inverse fluctuation conductivity $\bar{\sigma}_h^{-1}$ becomes an almost linear function for $\bar{\tau}\bar{\omega}$. For larger values of ϵ_h we find that the curves for $\bar{\sigma}_h^{-1}$ vs $\bar{\tau}\bar{\omega}$ tend more and more to the curve for $\bar{\sigma}_0^{-1}$.

In calculating the fluctuation conductivity, we have assumed for simplicity a single-pairing component. For several-pairing components we obtain coupled equations for the corresponding fluctuation components $\delta\Delta_i(\mathbf{r}, \omega)$, which are analogous to the linearized gap equations in Eq. (13) determining $H_{c2}(T)$ or $T_{c2}(H)$. The only difference is that the coefficient $[V_i N(0)]^{-1}$ on the left-hand side is replaced by $[V_i N(0)]^{-1} - i\tau_i$ where τ_i is the relaxation time of $\delta\Delta_i$. By solving these equations in analogy to Sec. II, one obtains the pair fluctuation propagator. It is clear that for $\omega = 0$ and decreasing T a pole occurs first in this fluctuation propagator at $T = T_{c2}(H)$, as it must be.

IV. DISCUSSION

The first interesting result of this paper is that two *in-plane* pairing components (here an *s*- and *d*-wave component) can give rise to an upward curvature of H_{c2} perpendicular to the *ab* plane. The reduced upper critical field,

$$h_{c2}^*(t) = h_{c2}(t) [dh_{c2}(t)/dt|_{t=1}]^{-1}, \quad t = T/T_{c1},$$

depends sensitively on the parameters of the theory, namely, T_{c2}/T_{c1} , $(v_2/v_1)^2$, and $(v_{12}/v_1)^2$. This can be seen from the curves (1)–(5) in Fig. 1. Curves (1) and (2) refer to $T_{c2}/T_{c1} = 0.92$ and 1.0, respectively, and to the same values of $(v_2/v_1)^2 = 1.9$ and $(v_{12}/v_1)^2 = 1.4$. Both curves fit the observed upward curvature of H_{c2} (see the experimental dots of Ref. 3) and yield values of 66 and 63 T, respectively, at zero temperature. In general the shape of the curve for $h_{c2}^*(t)$ does not depend sensitively on the ratio of transition temperatures T_{c2}/T_{c1} of the two pairing states. The effect of changing the squared ratios of effective Fermi velocities $(v_2/v_1)^2$ and $(v_{12}/v_1)^2$ for a given $T_{c2}/T_{c1} = 1$ can be seen from curves (2)–(5). It is interesting that curve (5) is identical to the curve for a pure 2D pairing state ($T_{c2}/T_{c1} = 1$, $v_2 = v_{12} = 0$) and yields $h_{c2}^*(0) = 0.6$ which should be compared with the well-known value of 0.72 for the 3D case (clean limit). We remark that in principle the effective Fermi velocities v_1 , v_2 , and v_{12} can be calculated from the effective 2D band $\epsilon(k_x, k_y)$ (Ref. 19) and the effect of impurity scattering can be taken into account.¹⁷

We hope that future experiments will decide whether the upward curvature of H_{c2} is an intrinsic property of high- T_c superconductors or if it is just a consequence of flux creep.^{3,6} In the former case we would have a strong indication that anisotropic pairing states mix in. Then we expect other interesting phenomena such as those that have been investigated for heavy-fermion superconductors, for instance, a rich spectrum of collective modes⁹ which could lead to measurable effects on ultrasonic attenuation.

We intend to extend our theory to the much more complicated case where the field is directed perpendicular to the c axis. This can be done in analogy to the existing theory for mixed *p*-wave pairing in layered superconductors.²¹ The aim is to predict H_{c2} at zero temperature by fitting the observed upward curvature of H_{c2} perpendicular to the c axis.³ The effects of paramagnetic limiting

and impurity scattering on H_{c2} can be treated more easily within the framework of the quasiclassical equations of Eilenberger²⁰ which have to be modified in analogy to the present theory to account for an anisotropic Fermi surface and for anisotropic pairing.

The second interesting result of this paper is the field dependence of the in-plane dc fluctuation conductivity for fields parallel to the c axis. In Fig. 2(a), we have plotted our results for the inverse reduced-fluctuation conductivity, $\tilde{\sigma}_h^{-1}(0)$ vs $\epsilon = \ln(T/T_c)$ for different reduced fields, $h = \xi_{x,y}(0)^2 2eH$. Notice that $\tilde{\sigma}_h^{-1}$ is actually a function of $\epsilon_h \equiv \ln[T/T_{c2}(H)] = \epsilon + h$ and that $\tilde{\sigma}_h^{-1} = 0$ at $T = T_{c2}(H)$, that is, at $\epsilon = -h$. One recognizes from Fig. 2(a) that for large values of ϵ_h the curve for $\tilde{\sigma}_h^{-1}$ becomes nearly parallel to the curve for the inverse Lawrence-Doniach fluctuation conductivity,¹² i.e., $\tilde{\sigma}_0^{-1}(0) = [\epsilon(\epsilon + \gamma)]^{1/2}$. Here γ is given by $\gamma = 4[\xi_z(0)/c]^2$ where $\xi_z(0)$ is the coherence length and c the dimension of the unit cell along the c axis. In principle the ratio $\xi_z(0)/c$ can be calculated from the effective 2D band $\epsilon(k_x, k_y)$. Again the effect of impurity scattering can be taken into account.¹⁷

One can recognize some similarity between the theoretical curves for $\tilde{\sigma}_h^{-1}$ in Fig. 2(a) and the measured resistivity curves in $\text{YBa}_2\text{Cu}_3\text{O}_{7-x}$ (Ref. 1) and $\text{GdBa}_2\text{Cu}_3\text{O}_{7-x}$ (Ref. 2) for \mathbf{H} parallel to the c axis. In particular, the observed temperature of zero resistance $T_{c2}(H)$ corresponds roughly to that temperature where $\tilde{\sigma}_h^{-1}(0) = 0$. Then $T_{c2}(H)$ would be given by the relation¹⁵ $[T_{c2}(H) = T_c]/T_c = h \approx -0.012H(T)$ where the latter estimate corresponds to the measured $\xi_{ab}(0) \approx 24 \text{ \AA}$ of Refs. 1 and 2. It is tempting to fit the long almost linear rise of the experimental resistivity curves as a function of temperature^{1,2} by the almost linear $\tilde{\sigma}_h^{-1}$ vs ϵ_h curves. This can be done by choosing an appropriate value of the parameter $\gamma = 4[\xi_z(0)/c]^2$ which determines the temperature for crossover from 2D to 3D behavior. In Fig. 2 we have chosen a value $\gamma = 0.08$ which is close to the values which have been used to fit the measured fluctuation conductivity in zero field.¹⁶ As has been shown in Sec. III, the fit of the measured paraconductivity in zero field by fluctuation conductivity¹⁶ can be improved by considering a nearest and a next-nearest-neighbor band term along the c axis. These two terms can account for the two different separation distances between the Cu-O sheets. We hope that future experiments can decide whether the observed broad resistive transition in a field is due to fluctuation conductivity or to flux creep.^{3,6}

The third interesting result of this paper is the frequency dependence of the in-plane ac fluctuation conductivity for fields parallel to the c axis. In Fig. 2(b) we have plotted our results for $\tilde{\sigma}_h^{-1}$ versus the reduced variable $\bar{\tau}\bar{\omega}$ for a fixed reduced temperature $\epsilon_h = 0.001$ and for various reduced fields h . One recognizes that for $h = 0$ and for small fields h the function $\tilde{\sigma}_h^{-1}(\bar{\tau}\bar{\omega})$ becomes nearly a linear function for $\bar{\tau}\bar{\omega} \gg (\epsilon_h + \gamma)$, and that for large h this function is quadratic in $\bar{\tau}\bar{\omega}$. In the limit $h \rightarrow 0$, $\gamma \rightarrow 0$, and $\epsilon_h \rightarrow 0$ one recovers the well-known result for an ordinary bulk superconductor, namely, that the inverse fluctuation conductivity is strictly proportional to the frequency. Just above the transition temperature $T_{c2}(H)$ (that is, $\epsilon_h = 0$)

the ac fluctuation conductivity will contribute significantly to the surface impedance, transmissivity, and reflectivity at microwave or infrared frequencies. We hope that our results can be tested by measurements of these quantities.

Finally, we discuss the contribution of fluctuations to the specific heat in the presence of magnetic fields. For a field lying parallel to the c axis we obtain from the Aslamazov-Larkin diagram and the pair-fluctuation propagator in Eq. (23) the specific-heat contribution

$$C_H = [k_B/4\pi c \xi_{x,y}(0)^2] \tilde{C}_h, \quad (32)$$

$$\tilde{C}_h = \sum_{N=0}^{\infty} 2h(\epsilon_h + 2hN + \frac{1}{2}\gamma) \times (\epsilon_h + 2hN)^{-3/2} (\epsilon_h + 2hN + \gamma)^{-3/2}. \quad (33)$$

The variables $\epsilon_h = \epsilon + h$, γ , and h have been defined in Eq. (26). In the limit $h \rightarrow 0$ we recover the previous zero-field result,¹⁷ i.e., $\tilde{C}_0 = [\epsilon(\epsilon + \gamma)]^{-1/2}$. For $(\epsilon_h + 2hN) \ll \gamma$ we recover the previous result for an ordinary bulk superconductor.²²

We have calculated numerically \tilde{C}_h as a function of ϵ_h for $\gamma = 0.08$ and for different fields h . For $h \rightarrow 0$ we obtain agreement with the analytic expression quoted above. For large values of h the $N = 0$ term in Eq. (33) becomes dominant which means that \tilde{C}_h diverges like $\epsilon_h^{-3/2}$ as $\epsilon_h \rightarrow 0$. In Fig. 3 we have plotted our results for $\tilde{C}_h(\epsilon_h) = \tilde{C}_h(\epsilon + h)$ versus $\epsilon = \ln(T/T_c) = (T - T_c)/T_c$ for different values of h .

In Refs. 14 and 23 the difference of the measured specific heats in zero and finite field H ($C_0 - C_H$) has been plotted versus temperature. For a fixed temperature, this difference is found to increase as H is increased, much more rapidly for \mathbf{H} parallel than for \mathbf{H} perpendicular to the c axis.¹⁴ One can recognize from Fig. 3 that for a fixed value of $\epsilon = (T - T_c)/T_c > 0$ the difference ($\tilde{C}_0 - \tilde{C}_h$) indeed increases as h is increased. Thus it may be possible that above T_c where only fluctuations should contribute to $(C_0 - C_H)$ the data can be fitted by choosing an

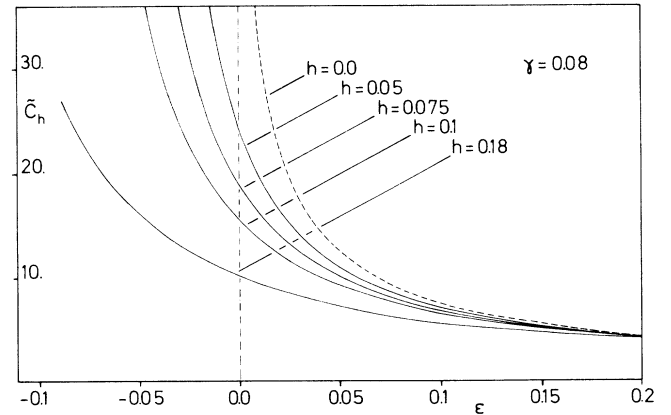


FIG. 3. Reduced fluctuation specific heat \tilde{C}_h [see Eq. (32)] vs $\epsilon = \ln(T/T_c)$, for 2D to 3D crossover parameter $\gamma = 0.08$ and for different reduced fields h . The divergence of \tilde{C}_h occurs at $\epsilon \rightarrow -h$ corresponding to $T \rightarrow T_{c2}(H)$. The field is directed along the c axis.

appropriate value of γ . Comparison with experiment below T_c is hampered by the fact that we do not know the fluctuation specific heat below $T_{c2}(H)$, in particular, that for zero field. Further, the theory predicts a divergence of \bar{C}_h at $\epsilon_h=0$, that is, at a temperature $T_{c2}(H) \approx T_c[1 - 0.012H(T)]$. This prediction seems to be in contradiction to experiment: According to the data of Ref. 14 the difference $(C_0 - C_H)$ at given field is almost constant as T is decreased while the data of Ref. 23 yield a kind of peak for this difference as T is decreased.

It is much more difficult to calculate the contributions of fluctuations to conductivity and specific heat for magnetic fields *perpendicular* to the c axis. First, one would have to solve the eigenvalue problem for the fluctuation propagator.¹⁵ This is complicated because the kernel of the differential operator of infinite order contains the

tight-binding band term $[\cos(cq_z) - 1]$. Second, one would have to consider the possibility of a pairing component along the c axis.

We hope that future experiments will decide whether or not our simple modifications of conventional BCS theory are adequate to describe high- T_c superconductivity.

ACKNOWLEDGMENTS

We would like to thank K. Scharnberg for helpful suggestions and discussions concerning the calculation of the upper critical field. We are indebted to the authors of Refs. 3, 14, and 16 for providing us with copies of their work prior to publication.

-
- ¹Y. Iye, T. Tamegai, H. Takeya, and H. Takei, *Jpn. J. Appl. Phys. Lett.* **26**, L1057 (1987).
²Y. Iye, T. Tamegai, H. Takeya, and H. Takei, *Physica B* **148**, 224 (1987).
³T. K. Worthington, W. J. Gallagher, D. L. Kaiser, F. H. Holtzberg, and T. R. Dinger, *Physica C* **153-155**, 32 (1988).
⁴B. Oh, K. Char, A. D. Kent, M. Naiko, M. R. Beasley, T. H. Geballe, R. H. Hammond, A. Kapitulnik, and J. M. Graybeal, *Phys. Rev. B* **37**, 7861 (1988).
⁵C. J. Lobb, *Phys. Rev. B* **36**, 3930 (1987); A. Kapitulnik, M. R. Beasley, C. Castellani, and D. Di Castro, *ibid.* **37**, 537 (1988).
⁶Y. Yeshurun and A. P. Malozemoff, *Phys. Rev. Lett.* **60**, 2202 (1988).
⁷K. Scharnberg and R. A. Klemm, *Phys. Rev. B* **22**, 5233 (1980).
⁸K. Scharnberg and R. A. Klemm, *Phys. Rev. Lett.* **54**, 2445 (1985); *J. Magn. Magn. Mater.* **54-57**, 381 (1986).
⁹H. Monien, K. Scharnberg, L. Tewordt, and N. Schopohl, *Phys. Rev. B* **34**, 3487 (1986); *J. Low Temp. Phys.* **65**, 13 (1986).
¹⁰P. Kumar and P. Wölffe, *Phys. Rev. Lett.* **59**, 1954 (1987).
¹¹R. A. Klemm, *J. Low Temp. Phys.* **16**, 381 (1974).
¹²J. Lawrence and S. Doniach, in *Proceedings of the Twelfth International Conference on Low Temperature Physics, Kyoto, 1970*, edited by E. Kanda (Keigaku, Tokyo, 1971), p. 361.
¹³H. J. Mikeska and H. Schmidt, *Z. Phys.* **230**, 239 (1970).
¹⁴K. Athreya, O. B. Hyun, J. E. Ostenson, J. R. Clem, and D. K. Finnemore (unpublished).
¹⁵P. A. Lee and M. G. Payne, *Phys. Rev. B* **5**, 923 (1972).
¹⁶S. J. Hagen, Z. Z. Wang, and N. P. Ong (unpublished).
¹⁷L. Tewordt, D. Fay, and Th. Wölkhausen, *Solid State Commun.* **67**, 301 (1988).
¹⁸M. Sigrist and T. M. Rice, *Z. Phys.* **B 68**, 9 (1987).
¹⁹V. J. Emery, *Phys. Rev. Lett.* **58**, 2794 (1987).
²⁰C. T. Rieck, Diplomarbeit, University of Hamburg, 1987 (unpublished); N. Schopohl (unpublished).
²¹R. A. Klemm and K. Scharnberg, *Phys. Rev. B* **24**, 6361 (1981).
²²P. A. Lee and S. R. Shenoy, *Phys. Rev. Lett.* **28**, 1025 (1972).
²³M. B. Salamon, S. E. Inderhees, J. P. Rice, B. G. Pazol, D. M. Ginsberg, and N. Goldenfeld, *Phys. Rev. B* **38**, 885 (1988).